

1 **Crustal Structure in the Southern Apennines**
2 **from Teleseismic Receiver Functions**

3 **Michael S. Steckler¹, Nicola Piana Agostinetti², Charles K. Wilson¹,**
4 **Pamela Roselli³, Leonardo Seeber¹, A. Amato² and A. Lerner-Lam¹**

5 ¹*Lamont-Doherty Earth Observatory of Columbia University, Palisades, NY 10964, USA*

6 ²*Istituto Nazionale di Geofisica e Vulcanologica, Centro Nazionale Terremoti, Roma, Italia*

7 ³*Istituto Nazionale di Geofisica e Vulcanologica, Osservatorio Sismologico Arezzo, Arezzo,*
8 *Italia*

9 *Keywords: thrust tectonics, Apennines, continental collision, seismology, receiver functions,*
10 *structural geology*

11 **Abstract**

12 While the upper crustal structure of the Southern Apennines is known, lack of control on
13 the deep structure allows competing thin-skin and thick-skin models of the orogen. In thin-
14 skin models the detachment decouples a stack of rootless nappes from the basement. In
15 thick-skin models, basement is involved in the most recent phase of thrusting. To examine
16 crustal structure, we use teleseismic data from the CAT/SCAN array in southern Italy. We
17 use receiver functions (RF) processed into a Common Conversion Point (CCP) stack to
18 generate images of the crust. Interpretation and correlation to geological structure is done
19 using inversions of individual station RFs. We focus on a shallow discontinuity where P-to-
20 S conversions occur. In the foreland, it corresponds to velocity jumps between carbonate
21 and clastic strata with basement. A similar interpretation for the Apennines provides the
22 most parsimonious explanation and supports a thick-skin interpretation. In a thick-skin
23 reconstruction, the amount of shortening is much smaller than for a thin-skin model. This
24 implies considerably less Plio-Pleistocene shortening across the Apennines and suggests an
25 E-SE motion of the Calabrian Arc subparallel to the southern Apennines rather than a
26 radial expansion of the Arc.

27 **Introduction**

28 The Southern Apennines (SA) results from impact of the continental Apulian Platform (AP)
29 with the Calabrian Arc (CA). Abundant outcrop, seismic and well data (e.g., Cello and Mazzoli,
30 1998) constrain the shallow part of the orogen. Here, large carbonate banks are involved in both
31 the allochthonous (Apenninic) and autochthonous (Apulian) parts of the SA. The Apenninic
32 units comprise large nappes that overthrust the AP, similar to many fold-and-thrust belts with
33 detached strata imbricated above basement. Beneath these nappes, the AP becomes involved in
34 the thrusting. However, seismic data, including recently published CROP lines (Scrocca et al.,
35 2005; Finetti et al., 2005) do not resolve whether basement is involved in the deeper thrusts.
36 Thin-skin reconstructions with imbricated AP units above a detachment (e.g., Mazzotti et al.,
37 2000) and thick-skin reconstructions with thrusts rooted in basement beneath the AP (Menardi
38 Noguera and Rea, 2000) are both viable. These geometries permitted imply large differences in
39 shortening. Thick-skin models require <30 km shortening of Apulia, while thin-skin models
40 imply >120 km shortening. This has significant implications for opening of the Tyrrhenian Sea.
41 Did the CA expand radially or primarily rollback towards the E or SE? What is the amount of
42 obliquity in the SA?

43 In 2003, we deployed a broadband seismic array, the Calabria-Apennine-

44 Tyrrhenian/Subduction-Collision-Accretion Network (CAT/SCAN) to image the SA, CA and the
45 transition between them (Fig. 1). We image the crust of the SA using receiver functions (Burdick
46 and Langston, 1977). Velocity boundaries within the crust produce partial conversions of
47 incoming P-waves to S-waves. We use CAT/SCAN data to map velocity discontinuities and use
48 this data for interpreting the structure of the SA.

49 **Geologic Setting**

50 During the Neogene, rollback renewed the oceanic lithosphere of the Western Mediterranean
51 (Malinverno and Ryan, 1986; Gueguen et al., 1998; Rosenbaum et al., 2002). First, the Corsica-
52 Sardinia block rifted off Europe and opened the Balearic Sea, but stalled at 17-18 Ma, possibly
53 due to collision with outer blocks of Apulia (Rosenbaum et al., 2002; Catalano et al., 2004).
54 Resumed rollback led to rifting of Calabria off Sardinia at 10-12 Ma and the opening of the
55 Tyrrhenian Sea (Malinverno and Ryan, 1986; Gueguen et al., 1998). During rollback of the CA,
56 the northern part of the arc progressively collided with Adria to create the Apennines and the
57 southern part obliquely collided with Africa to form the Maghrebides. Calabria and NE Sicily are
58 the only remaining part of the subduction zone still consuming oceanic crust (Fig. 1).

59 The SA is a stack of NE-verging thrust sheets with 4 major units. The uppermost is the
60 Ligurian Complex, a Jurassic-E. Miocene set of heterogeneous units that are the accretionary
61 complex of the former subduction zone (Catalano et al., 2004).

62 Structurally below is the Apennine Platform (ApP). It is primarily Triassic to Miocene
63 shallow-water carbonates and associated deposits (Cello and Mazzoli, 1998; Menardi Noguera
64 and Rea, 2000; Finetti et al., 2005). The ApP may have started as a Bahama-like set of carbonate
65 banks (Cello and Mazzoli, 1998; Ciarapica and Passeri, 2005) that formed the outer blocks of
66 Apulia. The ApP was eventually sheared off its basement as a set of rootless nappes.

67 Next is the Lagonegro Sequence, the cover of the deep-water basin separating the Apennine
68 Platform from Apulia. The lower Lagonegro sequence grades from Permian-E. Triassic rift basin
69 facies to deep-water facies (Mostardini and Merlini, 1986). The distinct upper sequence grades
70 from a L. Cretaceous deep-water facies to a Miocene terrigenous flysch and mélange.

71 Lowermost is the AP, the autochthonous basement in the foreland. The AP is composed of 5-
72 7 km of Triassic-Miocene shallow-water carbonates and dolomites overlying >1 km of Permian-
73 L. Triassic clastics. Well logs, including the 7070m Puglia-1 well (Fig. 1), indicate high
74 velocities for the AP, over a lower velocity for the basal clastics (Improta et al., 2000; DR4).

75 The Apennine-Lagonegro terranes were emplaced by Miocene thin-skin thrusting. The
76 shearing off of the AP from its basement may have enabled CA rollback to resume. Following
77 subduction of the Lagonegro oceanic(?) basin, the northern CA collided with the AP. The AP is
78 first cut by normal faults related to flexural bending, but then as it underthrusts the Apennines,
79 becomes offset by thrusts.

80 Well and seismic data constrain the structure of the Apennine-Lagonegro terranes. The top of
81 the AP is widely recognized but its base is only seen locally. Recent normal faults and
82 extensional basins on the Tyrrhenian side of the SA complicate the structure. As a result, two
83 contrasting end-member models (Fig. 2) both satisfy existing data: A thick-skin model where
84 thrusts involved Apulian basement since the late Pliocene-early Pleistocene (Menardi Noguera
85 and Rea, 2000; Finetti et al., 2005) and a thin-skin model where thrusts imbricate the AP, but do
86 not penetrate its basement (Mazzotti et al., 2000).

87 Butler et al. (2004) and Scrocca et al. (2005) discuss the merits of the two models but reach

88 opposite conclusions. For the thin skin, the allochthon is thickened by duplexing, requiring
89 shortening of 90-120 km (Mazzotti et al., 2000; Scrocca et al., 2005). This requires a significant
90 radial component of shortening during the rollback of the CA. The extra crust must either be
91 subducted or deformed farther west. For the thick skin, steeper thrust faults rooted in basement
92 require shortening of only 10-30 km (Menardi-Noguera and Rea, 2000; Butler et al., 2004;
93 Scrocca et al., 2005). The thick-skin model requires a change from the earlier thin-skin thrusting
94 when the CA encounters Apulia. Thus, the ApP collided with the CA and underwent thin-skin
95 shortening of ~200 km, while the larger AP underwent thick-skin shortening of tens of
96 kilometers.

97 **Seismic Data Analysis**

98 CAT/SCAN is a land (39 stations) and marine (12 stations) seismic experiment to image
99 crust and mantle structure beneath Calabria and its transition to the SA (Fig. 1). The deployment
100 from Dec. 2003-Oct. 2005 included linear arrays across the CA and SA and a regional grid
101 spanning the transition between the two areas.

102 We applied common conversion point (CCP) stacking of receiver functions (RF) (Dueker
103 and Sheehan, 1998; Wilson et al., 2004) using 95 events with $M_w > 6.0$ with epicentral distances
104 of 30° to 110° (Fig. DR1). RFs were produced by deconvolving P-phase vertical seismograms
105 from radial and transverse seismograms (Ligorria and Ammon, 1999). This procedure extracts
106 Ps, S waves converted from the P at refracting interfaces. The amplitude of the conversions
107 depends upon the impedance contrast across the interface and the incidence angle. A Ps phase
108 from the top of a low-velocity body will be reversed in polarity from the incident wave.

109 RFs from a single station span a range of azimuths and incidence angles illuminating
110 subsurface refractors at different points. To optimize this data, we depth migrated the radial
111 conversions along their raypaths and stacked them into CCP bins. The bins are 15×15 km across
112 and 0.5 km thick forming a volume $210 \times 315 \times 60$ km (Fig. 3, DR2). To fill empty bins we used a
113 smoothing algorithm averaging over distances inversely with data density. A regularized
114 inversion enforces smoothness in the absence of data. In the image, red are positive and blue are
115 negative conversions. A generic velocity model was used for the depth migrations, thus depth
116 errors up to several km are possible.

117 To get robust constraints on features of our CCP image along the linear SA array, we applied
118 a complementary single station RF inversion technique. We computed RFs using teleseismic
119 events with $M_w > 5.5$ to obtain maximum back-azimuth (baz) coverage (~60 RF per station). We
120 analyzed baz dependence of the RF datasets using harmonic expansion coefficients (HEC)
121 (Gilardin and Farra, 1998). Surface geology and the HEC were used as *a priori* information on
122 the velocity profile at each station. We inverted the RF data using the 2-stage NA approach
123 (Sambridge, 1999a,b), a Monte-Carlo inversion technique. In the first part, the dataset is
124 iteratively compared with synthetics computed from models sampling the parameter space. In the
125 second part, we use a Bayesian approach to obtain *a posteriori* probability distributions (PPD)
126 for each parameter, from which we compute statistical estimators. To compute synthetics from
127 3D structures, we coupled the NA with the RAYSUM code (Frederiksen and Bostock, 2000).
128 Details are in DR3.

129 **Results and interpretation**

130 The CCP volume images large-scale crustal structures below the SA. A number of high-
131 amplitude coherent features persist over large regions where station control is good. There are
132 also features of limited extent, some of them multiples. The CCP volume (Fig. 3, DR2) shows 3

133 strong Ps converters, which gently dip SW and are continuous throughout the illuminated parts
134 of the SA. We focus on the shallowest converter located at 8-11 km depth; it is located at the
135 bottom of the well-constrained structure of SA (see Scrocca et al. 2005) and is the most relevant
136 to the structural style of the Apennines. This conversion is continuous in parts of the CCP
137 volume and separated into 2 distinct surfaces elsewhere.

138 Calabria, in the lower left of Figure 3, exhibits a very different character without the strong
139 conversions seen in the SA. This fits the contrasting structure of Calabria, which is still
140 subducting oceanic crust and has not (yet) collided with Apulia. The transition between the SA
141 and Calabria has few coherent features. This is also the case for SKS splitting (Baccheschi et al.,
142 2007) and likely reflects a complex structure at the transition.

143 Figure 4 compares the CCP image and RF inversions to the geologic cross-sections. To
144 obtain the best resolution, we sampled the CCP volume along the transect of seismic stations
145 nearest the geologic sections (see Fig. 3). The strong positive conversion at 7-10 km is composed
146 of two separate features, beneath the foreland and under the Apennines. Elsewhere, off the
147 profile, they blend into a single surface.

148 The best constraints on the origin of this conversion come from CRBB in the AP (Fig. 4,
149 DR3). The Puglia-1 well provides geology and velocity constraints (≤ 7 km). The CRBB RF
150 shows little azimuthal dependence, consistent with the flat-lying AP, and can be modeled using a
151 1D S-velocity profile. The inversion yields velocity layering similar to the well. We find that a
152 low velocity corresponding to the clastic layer in the AP is required, and that AP layering is
153 composed of two main units with the deeper (dolomites) faster than the shallower (carbonates).
154 With this structure the RF (DR3) shows a strong positive pulse (red shallow conversion in CCP)
155 corresponding to the top of basement; the conversion from the base of the clastics overwhelms
156 negative conversion from its top. Moho is clear at 30 km, consistent with earlier estimates.

157 This correlation is reinforced by the inversion of VENO, which exhibits almost the same
158 structure beneath low-velocity foreland strata. The LVZ is not absolutely required, but is a
159 prominent feature of most models. RF inversions and the CCP clearly identify the structure of
160 the Apulian platform as it enters the orogen from the foreland.

161 The red CCP converter is lost where the AP plunges beneath the mountain belt. The RF for
162 the seismic stations (SX17, TRIC) at this position are complex due to 3D structure and cannot be
163 easily inverted.

164 Farther west in the Apennines, PICE shows a low velocity cover overlying layering similar to
165 the AP at the other stations (Fig. 4, DR3). PICE is situated in Lagonegro strata; the ApP only
166 extends that far farther north. Below the Lagonegro, the inversion yields layering almost
167 identical to VENO and CRBB. The thin LVZ is not fully resolved, but appears in most
168 inversions, including the mean model (DR3, Fig. 4). The LVZ is coincident with the decollément
169 between Apulia carbonates in the upper plate and the descending lower plate.

170 The inversion for POLA yields two LVZs. We identify the top one with the Lagonegro
171 clastics between the Apennines and Apulian carbonates (Fig. 4). The deeper LVZ correlates with
172 the red CCP converter. In the thick-skin model, this corresponds again to the basal clastics and
173 top of Apulian basement. In the thin-skin model, the signal arises from within the imbricated
174 Apulian carbonates. Again, the AP layers are nearly identical to the other stations.

175 The stations farther west are off section. The base of the ApP in the thick-skin model fits the
176 LVZ in SGIO because the profile and station are close and does not indicate this model is
177 preferred. Rather, it is evidence of the good fit of the RFs to the local geology. The most

178 significant result in SGIO and CAVE is shallow Moho at 23 and 21 km depth. This is shallower
179 than either of the geologic models but is consistent with other data indicating a shallow Moho on
180 the Tyrrhenian side of the SA (Piana Agostinetti et al., 2002). The Apulian layers are not seen in
181 the inversion, but would comprise almost the entire crust if present intact.

182 Consistency between the geology, RF inversions and CCP image on the AP foreland is
183 strong (Fig. 4; DR4). The LVZ required by the RF inversion gives rise to the red “horizon” on
184 the CCP image. This can be traced into the beginning of the foldbelt where the Apulia begins to
185 plunge downward.

186 The shallow parts of the SA also show a consistency between the geology and the RF
187 inversions (Fig. 4). Low near-surface velocities correspond to the foreland basin sediments and
188 Lagonegro strata. Higher velocities correspond to the ApP. LVZs at their base are seen in SGIO
189 and POLA.

190 At greater depth, the interpretations beneath the SA differ. For the thick skin model (Fig. 4c),
191 the LVZ corresponds to the base of AP carbonates and top of basement. The red converter in the
192 CCP is too shallow, perhaps due to the generic velocities used to convert the CCP to depth. For
193 the thin skin model (Fig. 4b), the LVZ and red converter lie in the midst of imbricated AP strata.
194 It is possible that there is a preserved low-velocity clastic horizon, but would have to be thick
195 and coherent enough to generate the conversions seen in the RF and CCP. Alternatively, the
196 thrusts could be thin skin, but without the imbrication so that the converter corresponds to the
197 base of the thrust sheet.

198 The stations on the Tyrrhenian side also have a well-defined Moho shallower than those in
199 either model. In the thin-skin model, the Apulian carbonates would extend down to the Moho. In
200 the thick-skin model, the Tyrrhenian stations are beyond the western edge of the AP. An initially
201 thin or tectonically thinned basement would underlie the Apennine nappes. Scrocca et al. (2005)
202 propose the formation of a shallower “New” Tyrrhenian Moho related to the Tyrrhenian
203 extension.

204 **Conclusions**

205 Both thin- and thick-skin models contain elements that fit and misfit CAT/SCAN seismic
206 data. We find that the thick-skin model is most consistent with the seismic data, requiring a
207 uniform explanation for the velocity boundaries producing the P-S conversions observed in the
208 RF. The consistent structure of the AP across the orogen is compelling. For the thin-skin model
209 to fit, the extent of imbrication of the AP must be drastically reduced, greatly lowering the
210 shortening estimates for the orogen. The low amount of shortening implied by the thick-skin
211 model suggests the CA primarily migrated to the E-SE and implies some obliquity to the orogen
212 (e.g., Rosenbaum and Lister, 2004). However, left-lateral deformation is known primarily from
213 late extension that and postdates thrusting (Catalano et al., 2004). The greater shortening of the
214 thin-skin model implies a more radial expansion of the CA, which may reflect the shape of the
215 circular Marsili basin in the eastern Tyrrhenian Sea. However, both models must better account
216 for the larger-scale descent of the Apulian plate into the mantle (Scrocca et al., 2005). Neither is
217 consistent with shallow Moho near the Tyrrhenian. Thus both models need to be fully integrated
218 with the 3D geometry of the subduction system.

219 **Acknowledgements**

220 This work was funded by US National Science Foundation grant EAR99-10554 and by INGV.
221 We thank all the participants in the CAT/SCAN fieldwork and L. Margheriti for a constructive
222 review. Data collection and archival were facilitated by IRIS. LDEO publication No. 7086.

223 1GSA Data Repository item 2005##, [brief description], is available online at
224 www.geosociety.org/pubs/ft2005.htm, or on request from editing@geosociety.org or Documents
225 Secretary, GSA, P.O. Box 9140, Boulder, CO 80301-9140, USA.

226 **References**

- 227 Baccheschi, P., Margheriti, L., and Steckler, M.S., 2007, Seismic Anisotropy reveals focused
228 mantle flow around the Calabrian slab (Southern Italy), *Geophys. Res. Lett.*, v. 34, p. L05302,
229 doi:1029/2006GL028899.
- 230 Burdick, L.J., and C.A. Langston, 1977, Modeling crustal structure through use of converted
231 phases in teleseismic body-wave forms, *Bull. Seismol. Soc. Amer.*, v. 67, p. 677-691.
- 232 Butler, R.W.H., S. Mazzoli, S. Corrado, M. De Donatis, D. Di Bucci, R. Gambini, G. Naso, C.
233 Nicolai, D. Scrocca, P. Shiner, and V. Zucconi, 2004, Applying thick-skinned tectonic
234 models to the Apennine thrust belt of Italy-Limitations and implications, in K. R. McClay,
235 ed., *Thrust tectonics and hydrocarbon systems: AAPG Mem.* 82, p. 647-667.
- 236 Catalano, S., C. Monaco, L. Tortorici, W. Paltrinieri and N. Steel, 2004, Neogene-Quaternary
237 tectonic evolution of the southern Apennines, *Tectonics*, v. 23, doi:10.1029/2003TC001512.
- 238 Cello, G. and Mazzoli, S. , 1998, Apennine tectonics in southern Italy: a review, *J. Geodyn.* v.
239 27, p. 191-211.
- 240 Ciarapica, G. and L. Passeri, 2005, Ionian Tethydes in the southern Apennines, in CROP
241 PROJECT: Deep Seismic Exploration of the Central Mediterranean and Italy, *in* I.R. Finetti,
242 ed., Elsevier, Amsterdam, p. 209-224.
- 243 Dueker, K.G., and Sheehan, A.F., 1998, Mantle discontinuity structure beneath the Colorado
244 Rocky Mountains and High Plains: *J. Geophys. Res.*, v. 103, p. 7153-7169.
- 245 Finetti, I.R., F. Lentini, S. Carbone, A. Del Ben, A. Di Stefano, P. Guarnieri, M. Pipan, and A.
246 Prizzon, 2005, Crustal tectono-stratigraphy and geodynamics of the southern Apennines from
247 CROP and other integrated geophysical-geological data, in CROP PROJECT: Deep Seismic
248 Exploration of the Central Mediterranean and Italy, *in* I.R. Finetti, ed., Elsevier, Amsterdam,
249 p. 225-262.
- 250 Frederiksen, A.W. and M.G. Bostock, 2000, Modelling teleseismic waves in dipping anisotropic
251 structures, *Geophys. J. Int.*, v. 141, p. 401-412.
- 252 Gilardin, N. and V. Farra, 1998, Azimuthal anisotropy in the upper mantle from observation of
253 P-to-s converted phases: application to southeast Australia, *Geophys. J. Int.*, v. 133, p. 615-
254 629.
- 255 Gueguen, E., Doglioni, C and Fernandez, M. , 1998, On the post-25 Ma geodynamic evolution of
256 the western Mediterranean, *Tectonophys.*, v. 298, p. 259-269.
- 257 Improta, L., G. Iannaccone, P. Capuano, A. Zollo and P. Scandone, 2000, Inferences on the
258 upper crustal structure of Southern Apennines (Italy) from seismic refraction investigations
259 and subsurface data, *Tectonophys.*, v. 317, p. 273-297.
- 260 Ligorria, J.P., and C.J. Ammon, 1999, Iterative deconvolution and receiver-function estimation,
261 *Bull. Seismol. Soc. Amer.*, v. 89, p. 1395-1400.
- 262 Malinverno, A. and W.B.F. Ryan, 1986, Extension in the Tyrrhenian Sea and shortening in the
263 Apennines as a result of arc migration derived from sinking of the lithosphere, *Tectonics*, v. 5,
264 p. 227-245.
- 265 Mazzotti, A., E. Stucchi, G. Fradelizio, L. Zanzi, and P. Scandone, 2000, Seismic exploration in
266 complex terrains: A processing experience in the southern Apennines, *Geophysics*, v. 65, p.
267 1402-1417.
- 268 Menardi Noguera, A., and G. Rea, 2000, deep structure of the Campanian-Lucanian Arc
269 (Southern Apennine, Italy), *Tectonophys.*, v. 324, p. 239-265.
- 270 Mostardini, F., and S. Merlini, 1986, Appennino centro meridionale, sezioni geologiche e
271 proposta di modello strutturale, *Memorie della Società Geologica Italiana*, v. 35, p. 177-202.
- 272 Piana Agostinetti, N., F.P. Lucente, G. Selvaggi and M. Di Bona, 2002, Crustal structure and
273 Moho geometry beneath the Northern Apennines (Italy), *Geophys. Res. Lett.*, v. 29, p. 1999.

274 Rosenbaum, G., Lister, G.S. and Duboz, C., 2002, Reconstruction of the tectonic evolution of the
275 western Mediterranean since the Oligocene. *J. Virtual Explorer*, v. 8, p. 107-126.
276 Rosenbaum, G., and G.S. Lister, Neogene and Quaternary rollback evolution of the Tyrrhenian
277 Sea, the Apennines, and the Sicilian Maghrebides, *Tectonics*, v. 23, p. TC1013,
278 doi:10.1029/2003TC001518, 2004
279 Sambridge M. , 1999a, Geophysical inversion with a neighbourhood algorithm -I. Searching a
280 parameter space, *Geophys. J. Int.*, v. 138, p. 479-494.
281 Sambridge M. , 1999b, Geophysical inversion with a neighbourhood algorithm -II Appraising
282 the ensemble, *Geophys. J. Int.*, v. 138, p. 727-746.
283 Scrocca, D., E. Carminati and C. Doglioni, 2005, Deep structure of the southern Apennines,
284 Italy: Thin-skinned or thick-skinned? *Tectonics*, v. 24, p. TC3005,
285 doi:10.1029/2004TC001634.
286 Wilson, C.K., C.H. Jones, P. Molnar, A.F. Sheehan, O.S. Boyd, 2004, Distributed deformation in
287 the lower crust and upper mantle beneath a continental strike-slip fault zone: Marlborough
288 fault system, South Island, New Zealand, *Geology*, v. 32, p. 837–840, doi:
289 10.1130/G20657.1.

290 **Figure 1.** Map of the CAT/SCAN seismic array. An active Wadati-Benioff zone to 500 km
291 depth is present only beneath the CA where oceanic crust is subducted. In the SA, the arc has
292 collided with the AP. We use events recorded by the array to examine the crustal structure of the
293 region in the box.

294
295 **Figure 2.** Contrasting interpretations of the SA. A) Thin-skinned model with rootless nappes of
296 AP detached from the basement (Mazzotti et al., 2000). B) Thick-skinned model with basement
297 involved thrusting (Menardi Noguera and Rea, 2000). C) Geology of southern Apennines with
298 the lines of the two sections (modified from Ciarapica and Passeri, 2005). Overall figure
299 modified from Scrocca et al. (2005).

300
301 **Figure 3.** Perspective image of CCP volume. Cutaway shows strong continuous features across
302 the SA and change in character at the SA-CA transition. Dots are CAT/SCAN stations and
303 dashed line is Apennine thrust front. Stations used for RF inversions are labeled. Map shows
304 piercing points for rays used in CCP image, geologic sections and CCP section.

305
306 **Figure 4. A)** Results of the RF inversions along profile (Fig. 3). Red lines show correlations (top
307 and base Apulia–solid; base Apennine–dashed). Thin **(B)** and Thick **(C)** skin geological models
308 with CCP image and RF inversions. In RF profiles, Apulian carbonates are filled and heavy line
309 is Moho. Detachment is shown by black-white line. P-velocities of Puglia-1 well are also shown.
310 See text for discussion.

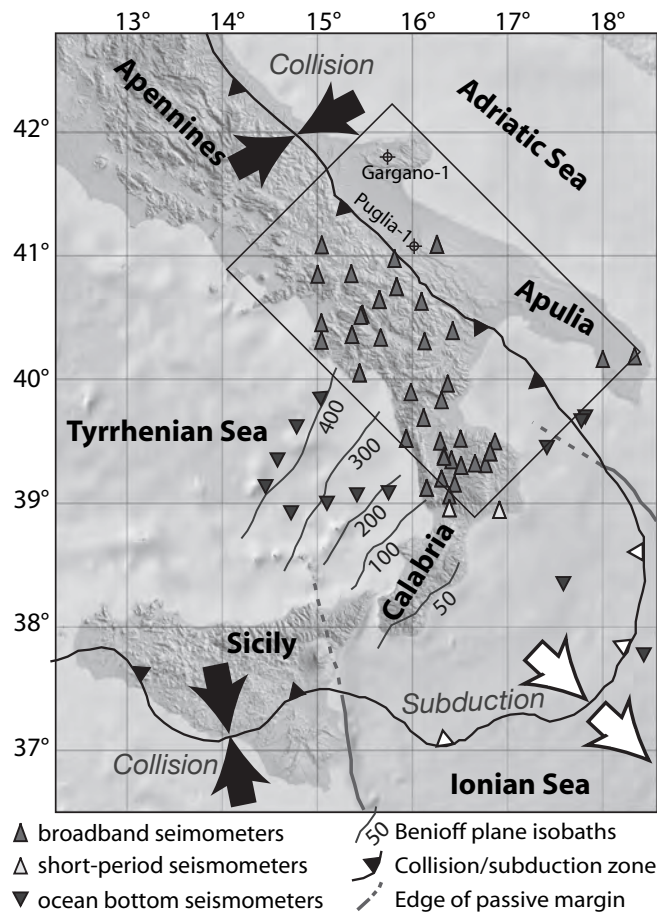


Figure 1

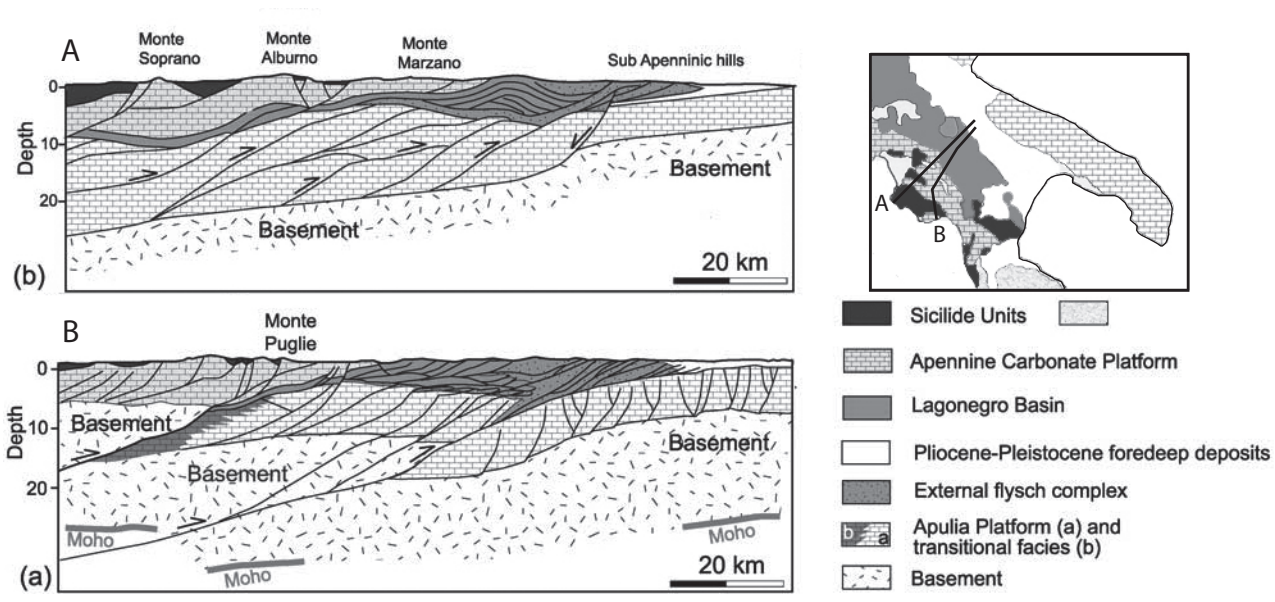


Figure 2

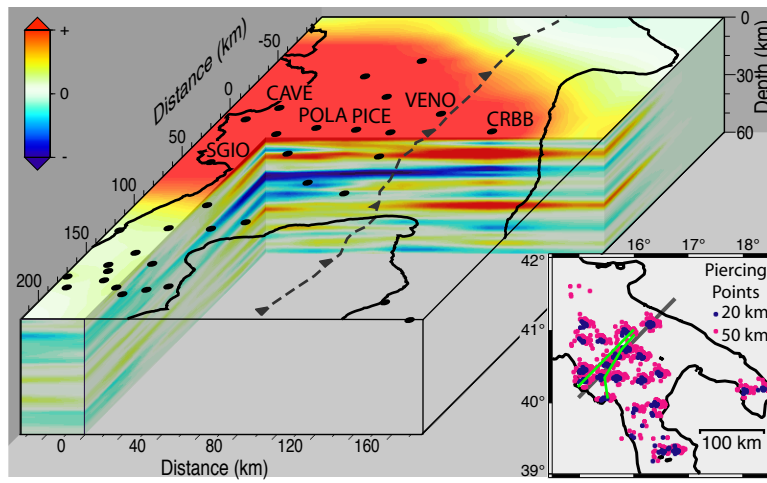


Figure 3

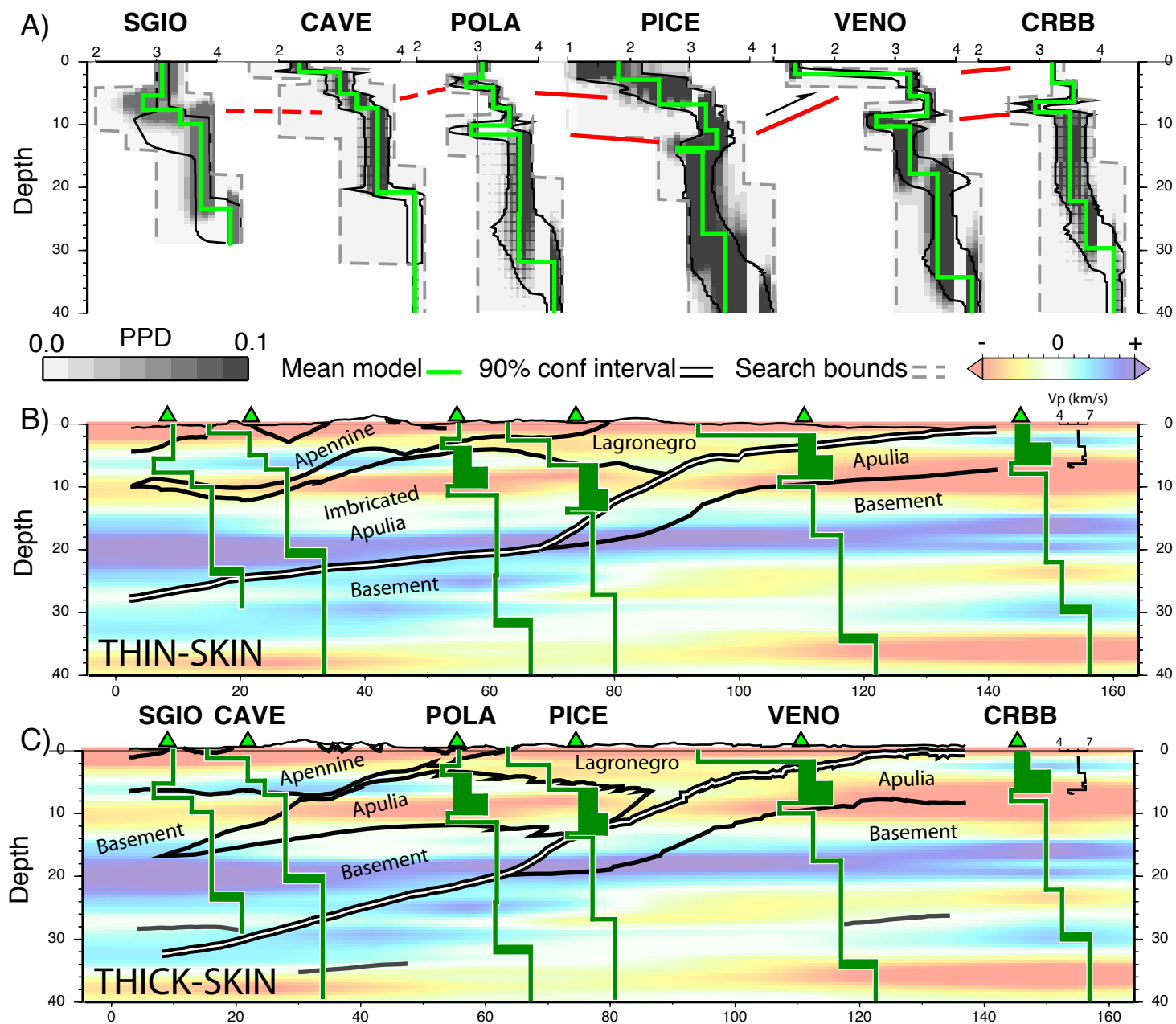


Figure 4